Baku State University Journal of Chemistry and Material Sciences, 2024, v. 1 (4), p.13-18

journal homepage: *http://bsuj.bsu.edu.az/en*
https://doi.org/10.30546/209501.201.2024.1.04.055

SYNTHESIS AND INVESTIGATION OF $Cd_xCu_{1-x}S$ AND $Zn_xCu_{1-x}S$ (x=0.5; 0.25 and 0.75) NANOCRYSTALS INTO FNBR MATRIX

Ofeliya Balayeva, Abdulsaid Azizov, Rasim Alosmanov
Baku State University, Baku, Azerbaijan

Received: 07 november 2024
Accepted: 10 december 2024
Published: 24 december 2024

$Cd_xCu_{1-x}S$ and $Zn_xCu_{1-x}S$ (x=0.5; 0.25 and 0.75) nanocrystals have been synthesized into functional nitrile butadiene rubber (FNBR) matrix. The structural and optical properties of obtained nanocomposites are investigated by X-ray diffractometer (XRD) and UV–visible spectroscopy. The effects of SILAR cycles and Cd(Zn)/Cu ratio on the formation of the crystals and their band gap has been studied in detail. The photocatalytic efficiency of FNBR based ternary nanocomposites of CuCd and CuZn sulfides were estimated towards the photodegradation of Malachite green dye under visible light irradiation. The average crystallite size and band gap of the obtained CdCuS and ZnCuS nanoparticles were calculated via Scherrer and Tauc equations, respectively. The Tauc equation from the absorbance data for $Cd_{0.5}Cu_{0.5}S$/FNBR and $Zn_{0.5}Cu_{0.5}S$/FNBR nanoparticles are ~3.64 eV and ~3 eV, respectively. $Cd_{0.5}Cu_{0.5}S$/FNBR and $Zn_{0.5}Cu_{0.5}S$/FNBR nanocomposites show 2 or 4 band gap values on the same Tauc plot. As seen in XRD, mixed crystal phases and defects also occurred on the ternary sulfide formation. Photodegradation of cationic dye shows that ternary metal sulfide nanocomposites are very good photocatalyst under visible light irradiation.

Keywords: Ternary metal sulfides; nanoparticles, nanocomposites, SILAR method, photodegradation

INTRODUCTION

Chalcogenide semiconductors synthesized in polymer matrices have high potential in the electronics and catalysis sectors of industry, mainly because they consist of a composition with both organic and inorganic components. Chalcogenide semiconductor nanostructures have been widely applied in photovoltaic cells, optical devices, diodes, and catalysis due to their tunable optical sensitivity, long fluorescence lifetime, and controllable composition Electrodeposited CuS, In_2S_3 and CdS thin films were successfully synthesized and investigated for H_2 production and CO_2 reduction [1]. The average crystallite sizes of these thin films were 55.99 nm, 50.37 nm and 63.51 nm, with 1.55 eV, 1.91 eV and 2.41 eV band gap energies, respectively. Authors highlight the critical role of band gap, surface morphology and crystallite size on the efficiency of CO_2 reduction and H_2 production. ZnS, [2], CdS [3], CoS [4] and NiS [5] and their heterostructures with CuS have attracted great interest due to their high energy storage capacity, interesting crystal structure, morphology, large surface area and different electronic states. The lattice defects formed during synthesis and their uniform and non-uniform distribution within and around the crystal lattice make them important for energy applications. Various transition metal sulfides containing CuS in their heterostructure play an important role in improving the charge storage capacity in supercapacitors. One of the main reasons for this is that these sulfides work synergistically with CuS. By creating a unity of p-n conductivity at the interface CuS and CdS, it is possible to increase the movement of photoexcited electrons. A heterostructure of CuS@CdS

E-mail address: ofeliyabalayeva@bsu.edu.az

nanocomposite shows high-specific capacitance (543.6 Fg^{-1} at 1 Ag^{-1}) with a very good rate capability and significant cycling stability [6].

The alloying element of zinc added to Cu1.8S enhances the thermoelectric properties, where pure P-type CuS transforms into N-type semiconductor and exhibits significantly improved electrochemical reaction performance [7], [8]. The intercalation of ZnCuS nanocrystallites into functionalized boron nitride (f-BN) layers creates porous structure that facilitates ion and electron transport [9]. The interaction between f-BN matrix and ZnCuS nanoparticles significantly exceeds their individual properties in electrocatalysis. The f-BN@ZnCuS composite exhibits high electrocatalytic activity, conductivity, and surface activity, making it a promising material for key components of sensors. The f-BN/ZnCuS nanocomposite based electrochemical sensors were effectively applied to the measuring of the concentrations of sulfadiazine in real samples [9].

EXPERIMENTAL

Functionalized nitrile butadiene rubber (FNBR) was used as a stabilizing agent and its preparation by the method of chemical transformation of polymers was shown in our previous works [10]. $CuCl_2 \cdot 2H_2O$, $CdCl_2 \cdot 2.5H_2O$, $ZnCl_2 \cdot 2.5H_2O$ and $Na_2S \cdot 9H_2O$ salt solutions were used as metal ion and sulfidizing precursors in the absorption and reaction steps of the SILAR method for the synthesis of $Cd_xCu_{1-x}S$ and $Zn_xCu_{1-x}S$ nanoparticles into FNBR matrix. The SILAR synthesis reaction of nanoparticles was carried out in 3, 5, 10, and 15 cycles and at 20mM and 50 mM concentrations of metal ions. Malachite green (MG) ($C_{23}H_{25}ClN_2$) cationic dye is used for the photodegradation experiments.

The obtained ternary sulfide/polymer nacomposites were characterized by X-ray diffractometer (XRD) (Bruker D2 Phaser), Infrared spectroscopy (FTIR) and Ultraviolet-visible spectrophotometer (UV-vis) (Specord 250).

RESULTS AND DISCUSSION

1.1 Structural properties by XRD.

The XRD results of of $Cd_{0.5}Cu_{0.5}S$ and $Zn_{0.5}Cu_{0.5}S$/FNBR nanocomposites obtained at different cycles and precursor concentration are given in Figure 1. The width diffraction peak observed at 2θ=~20° indicates the polymer matrix (FNBR) [10]. As can be seen, some binary phases of CuS, Cu_2S, ZnS and CdS are also obtained along with $Cd_{0.5}Cu_{0.5}S$ and $Zn_{0.5}Cu_{0.5}S$ ternary sulfides. The diffraction peaks for $Cd_{0.5}Cu_{0.5}S$ at lower SILAR cycles are three intense peaks (111), (220), (311) belonging to CdS and are observed at a slightly higher angle. With increasing number of cycles (15), the peaks mainly corresponded to CuS and were observed at slightly higher angles. The higher supersaturation and lower nucleation rate of CuS compared to CdS resulted in CdS dominating on the formation of ternary sulfide at low cycles. As the number of cycles increased, with the CuS crystal lattice becoming the basis, the particle growth rate increased. The average size of $Cd_{0.5}Cu_{0.5}S$ nanocrystallites was 2 and 29 nm at 5 and 15 cycles, respectively. In the formation of $Zn_{0.5}Cu_{0.5}S$ nanoparticles, along with ternary sulfide [11], many extraneous phases (binary sulfides and oxides) were also formed. Since zinc is more active than Cu and Cd, partial oxidation also occurred on its surface. The average size of $Zn_{0.5}Cu_{0.5}S$ nanocrystallites was 4.21 and 3.44 nm at 5 cycles using of 20mM and 50 mM concentrations of metal ions, respectively.

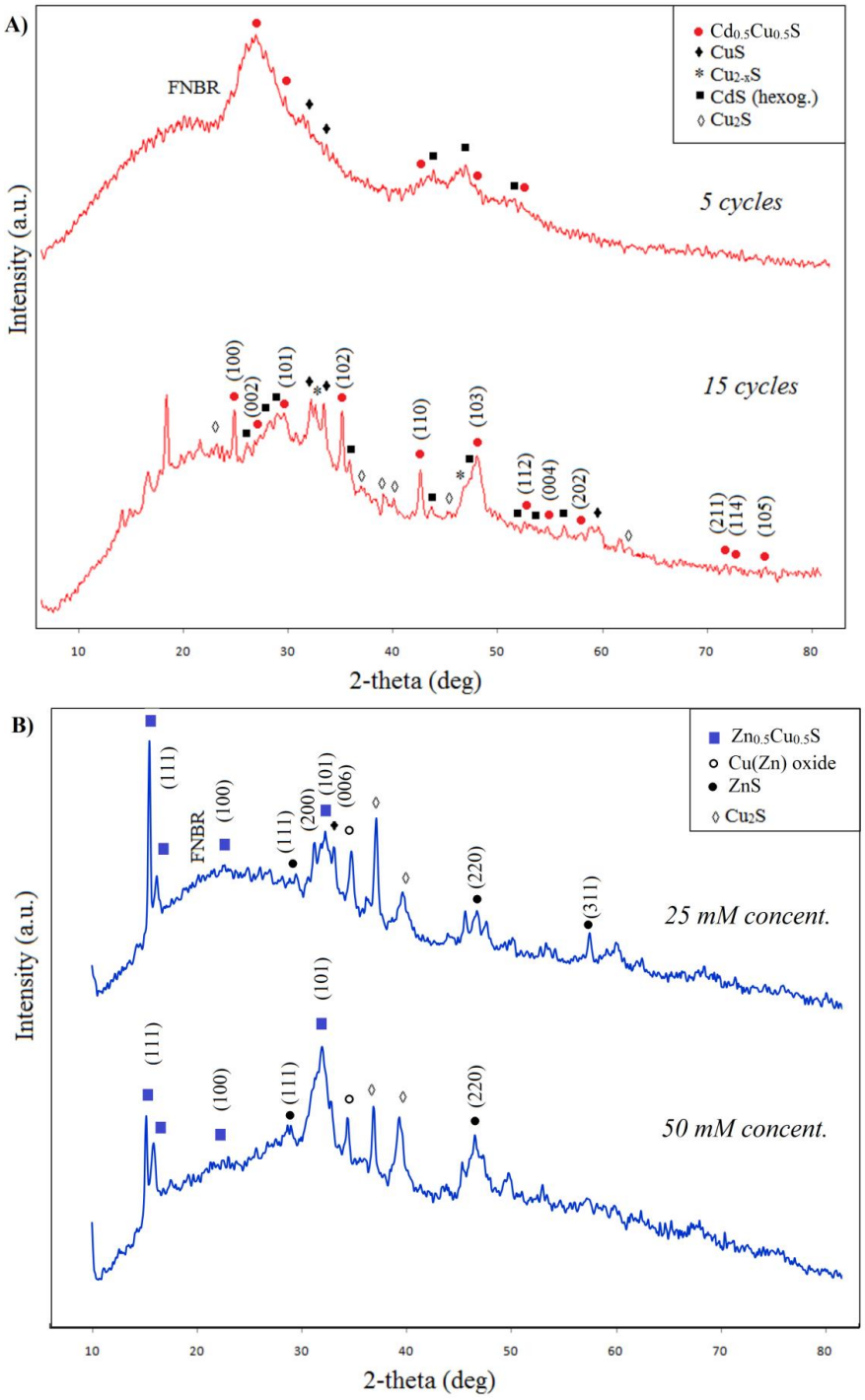

Fig.1. XRD patterns of $Cd_{0.5}Cu_{0.5}S$ and $Zn_{0.5}Cu_{0.5}S$/FNBR nanocomposites obtained at different cycles and precursor concentration.

3.2. Optical properties by UV-Vis

The absorbance (A) and transmittance (T%) spectra nanocomposite were obtained by UV–vis spectroscopy. Band gap (E_g) and Urbach (E_U) energy of the nanocomposites were estimated using Tauc equation [12] are shown in Figure 2. The $Cd_{0.5}Cu_{0.5}S$/FNBR nanocomposite show high bandgap energy as 3.7, 3.6 and 3.5eV by Tauc's plot obtained by 3, 5 and 15 cycles, respectively. It also show 2.3, 2.2 and 2.1 eV low bandgap energy by Tauc's plot for by 3, 5 and 15 cycles, respectively which are also greater than other analogs. It is possible for a single sample to show multiple band gap values on the same Tauc plot —

and that can actually tell as something very interesting about the material. Because samples contain more than one crystal phase**,** each with its own band gap. Having two or more band gaps also says that the nanocomposite contains different crystal phases. Here, $Cd_{0.5}Cu_{0.5}S$/FNBR and $Zn_{0.5}Cu_{0.5}S$/FNBR nanocomposites show 2 or 4 band gap values on the same Tauc plot. As seen in XRD, mixed crystal phases and defects also occurred on the ternary sulfide formation.

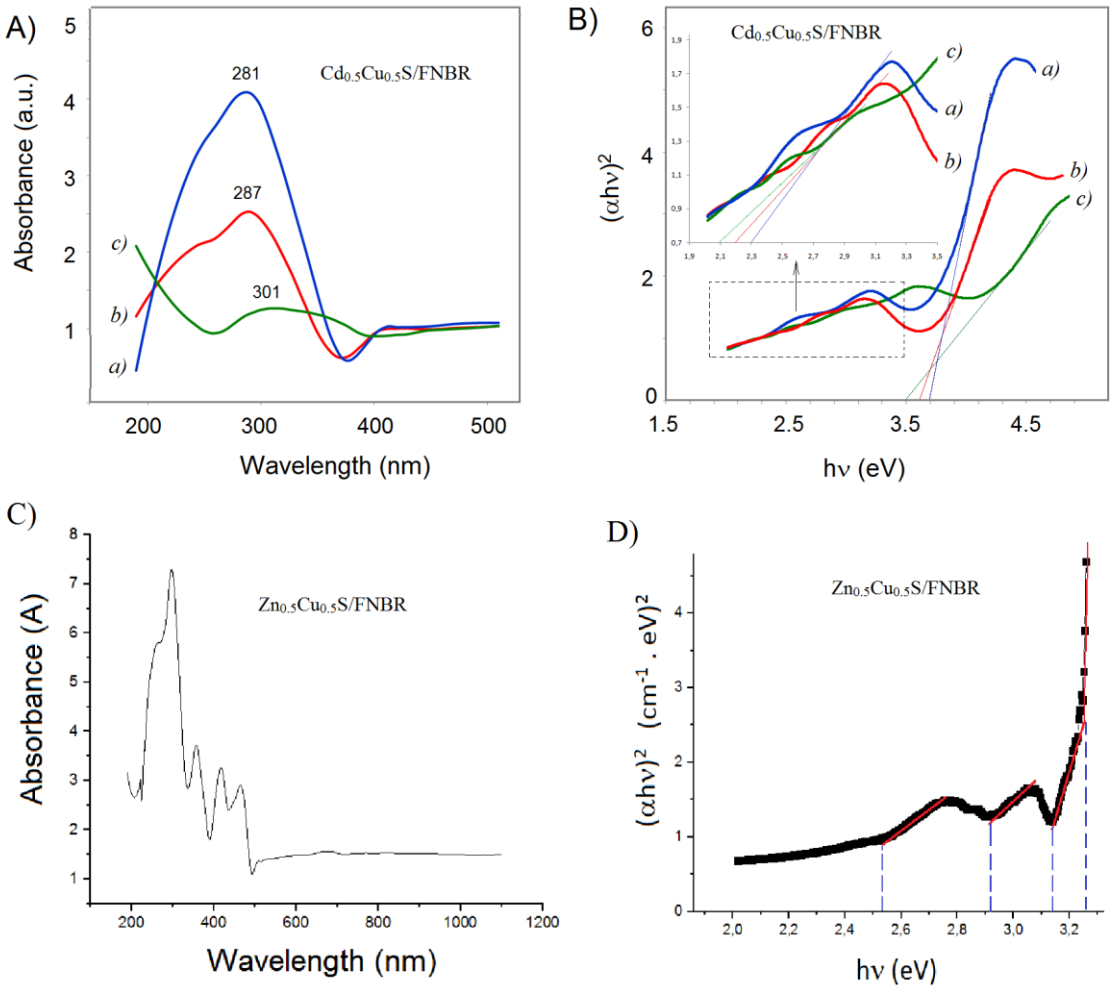

Fig.2. Optical UV–vis absorbance and band gap of $Cd_{0.5}Cu_{0.5}S$/FNBR and $Zn_{0.5}Cu_{0.5}S$/FNBR nanocomposite obtained after 3 (a), 5 (b) and 15 (c) cycles.

3.3 Photocatalytic application

The photocatalytic efficiency of the $CuCdS_2$/FNBR nanocomposite is estimated by using the photodegradation of malachite green. The obtained nanocomposites synthesized by the 5 cycles, photodegrades the malachite green 93.75% during 30 min. under visible light irradiation. The same result happened during 300 min by the $CuCdS_2$/FNBR nanomaterial synthesized by 15 cycles. As can be seen, photodegradation efficiency increased by 10 times with a very small particle size (~2 nm). However, the band gap of the nanocomposites obtained in 5 and 15 cycles is 2.3, and 2.1 eV, respectively. The main reason is although the size difference of the particles obtained by 5 cycles and 15 cycles is large; there was no sharp difference in the bandgap. Due to the large surface energy in small sized particles, the photodegradation rate is high. The probable mechanism of malachite green photodegradation is described as following:

$CuCdS_2/FNBR + h\nu \rightarrow CuCdS_2\,(h_{VB}^{+} + e_{CB}^{-})/FNBR$

$O_2 + e^- \rightarrow O_2\cdot^-$

$H_2O + h^+ \rightarrow \cdot OH + H^+$

$H_2O + O_2\cdot^- \rightarrow H_2O_2$

$H_2O_2 \rightarrow 2\ OH\cdot$

$C_{23}H_{25}ClN_2 + CuCdS_2/FNBR\ \text{chemisorb.} \rightarrow CuCdS_2/FNBR^- + C_{23}H_{25}N_2^+ + Cl^-$

$CuCdS_2/FNBR^- + C_{23}H_{25}N_2^+ + \cdot OH\ (O_2\cdot^-, HOO\cdot, \text{or } h+) \rightarrow \text{degradation product } H_2O + O_2$

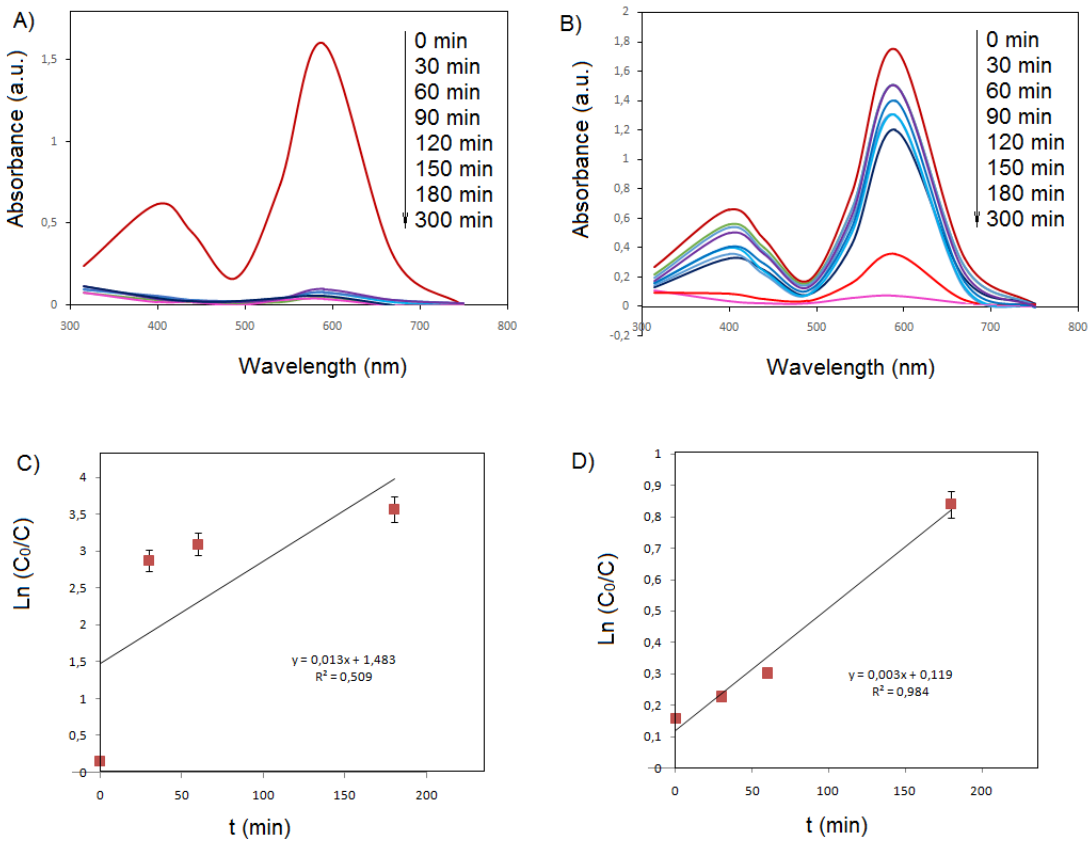

Fig. 3. Photocatalytic activity of the $CuCdS_2$/FNBR nanocomposite towards Malachite green.

CONCLUSION

$Cd_xCu_{1-x}S$/FNBR and $Zn_xCu_{1-x}S$/FNBR (x=0.5; 0.25 and 0.75) nanocomposites have been synthesized. Optical and structural properties of nanocomposites have been studied in detail. The average size of $Cd_{0.5}Cu_{0.5}S$ nanocrystallites was 2 and 29 nm at 5 and 15 cycles, respectively. Since zinc is more active than Cu and Cd, partial oxidation also occurred on its surface. The average size of $Zn_{0.5}Cu_{0.5}S$ nanocrystallites was 4.21 and 3.44 nm at 5 cycles using of 20mM and 50 mM concentrations of metal ions, respectively. The photocatalytic efficiency of the $CuCdS_2$/FNBR nanocomposite is estimated by using the photodegradation of malachite green. The obtained nanocomposites synthesized by the 5 cycles, photodegrades

the malachite green 93.75% during 30 min. under visible light irradiation. The same result happened during 300 min by the $CuCdS_2$/FNBR nanomaterial synthesized by 15 cycles.

REFERENCES

[1] Elrouby, M.; Gelany A.; Saber, H. Potentiostatic electrodeposition of copper, indium, and cadmium sulfides for CO_2 electroreduction: A path toward sustainable hydrogen generation, *International Journal of Hydrogen Energy*, 2024. 91, p. 877-892. https://doi.org/10.1016/j.ijhydene.2024.10.190

[2] Balu, R.; Sagedevan, S.; Dakshanamoorthy, A. A cost effective, facile hydrothermal approach of zinc sulfide decorated on graphene nanocomposite for supercapacitor applications. *J Nanoscience and Nanotechnology,* 2019. 19 (11), p. 6987-6994. https://doi.org/10.1166/jnn.2019.16670

[3] Balayeva, O.O.; Azizov, A.A.; Muradov, M.B.; Alosmanov, R.M.; Eyvazova, G.M.; Gahramanli, L.R., Mammadyarova, S.J.; Gasimov, R.J.; Bayramov M.A. Synthesis, structural and optical characterization of $Cd_xZn_{1-x}S$/FNBR nanocomposites. *ChemistrySelect,* 2024. 9 (9), p. e202305195. https://doi.org/10.1002/slct.202305195

[4] Balayeva, O.O.; Azizov, A.A.; Muradov, M.B.; Maharramov, A.M.; Eyvazova, Synthesis and characterization of cobalt sulfide/FNBR nanocomposites by SILAR method. *Journal of Ovonic Research*, 2016. 12(6), p.1-6. https://www.chalcogen.ro/267_BalayevaO.pdf

[5] Balayeva, O.O.; Azizov, A.A.; Muradov, M.B.; A.M.; Eyvazova, Dielectric characterization of CuxS-NiySz/FNBR and CuS-NiySz/FNBR nanocomposites. *Solid-State Electronics*, 2017. 132, p. 31-38. https://doi.org/10.1016/j.sse.2017.03.005

[6] Balu, R.; Panneerselvam A., Rajabathar, J.R.; Devendrapandi G. Synergistic effect of Echinops flower-like Copper sulfide@Cadmium sulfide heterostructure for high-performance all-solid-state asymmetric supercapacitor. *Journal of Energy Storage,* 2023. 72, p. 108447. https://doi.org/10.1016/j.est.2023.108447

[7] Sankar, G.; Saminathan, M. Perumal, S.; Arunachalam G.Thermoelectric properties of aliovalent Zn doped $Cu_{1.8}S$ polycrystalline materials. *Ceramics International,* 2024. 50, p. 13400-13411. https://doi.org/10.1016/j.ceramint.2024.01.252

[8] Wang, P.; Gao, Y.; Li, P.; Zhang, X.; Niu, H.; Zheng, Z. Doping Zn^{2+} in CuS nanoflowers into chemically homogeneous $Zn_{0.49}Cu_{0.50}S_{1.01}$ superlattice crystal structure as high-efficiency n-type photoelectric semiconductors. *ACS Appl. Mater. Interfaces,* 2016, 8, p. 15820-15827. https://pubs.acs.org/doi/10.1021/acsami.6b04378

[9] Gopal, N.; Ravikumar, N.K.; Perumal, P. Exploring the synergistic effect of functionalized boron nitride on zinc copper sulfide for enhanced electrochemical detection of sulfadiazine. *Surfaces and Interfaces,* 2025. 58, p. 105839. https://doi.org/10.1016/j.surfin.2025.105839

[10] Balayeva, O.O.; Azizov, A.A.; Muradov, M.B.; Alosmanov, R.M.; Eyvazova, G.M.; Gahramanli, L.R., Mammadyarova, S.J.; Gasimov, R.J.; Bayramov M.A. Synthesis and characterization of $Cu_xCd_{1-x}S$ nanocrystals into functionalized nitrile butadiene rubber matrix. *Journal of the Chinese Chemical Society,* 2024. 71 (6), p. 550-565. https://doi.org/10.1002/jccs.202300454

[11] Efe, F.O.; Olofinjana, B.; Fasakin, O.; Adebisi, C.A.; Eleruja, M.A.; Fabunmi, T.G. Opto-electronic properties of copper-zinc-sulfide thin films grown via metalorganic-chemical vapor deposition technique at different flow rates, *Physica Scripta* , 2023. 98, p. 085914. https://iopscience.iop.org/article/10.1088/1402-4896/ace2f8

[12] J. Tauc, A. Menth, States in the gap, *J. Non. Cryst. Solids*. 1972. 8–10, p. 569–585. https://doi.org/10.1016/0022-3093(72)90194-9